Sulfur in bulk rock and igneous apatite; tracing mineralized and barren trends in intrusions

by *Robert Frei[1]*

Abstract

The importance of elevated fO_2 levels in cooling magmas and during subsequent separation of aqueous fluids as one of the parameters controlling the potential to form genetically related sulfide mineralizations has long been recognized. This study aimed at testing whether or not the ratio of oxidized to reduced trace sulfur in bulk rock and apatite from Tertiary mineralized and barren intrusions in the Serbomacedonian Massif (Northern Greece) can be used as an indicator for initial fO_2 in the magmas and thus for tracing the potential of these intrusions to produce a mineral deposit. Both sulfur components were successfully extracted by the "Kiba"-technique (determination of concentration and isotope composition of both sulfur components in the same aliquot). Bulk rock sulfur is characterized by erratic SO_4^{2-}-derived / S^{2-}-derived sulfur concentration ratios (range from 0.12 to 4.75) and unsystematic $\delta^{34}S(S^{2-})$ and $\delta^{34}S(SO_4^{2-})$ varying from –6.51 to +2.53 and from –0.57 to +8.67 per mil, respectively. These data cannot be used to distinguish barren from mineralized trends because they seem preturbated by later disturbances induced by superposed propylitic alteration. Apatite, in contrast, resisted post-magmatic alteration and preserved its initial sulfur concentration, which in barren intrusions ranges from 400 to 575 ppm and in potentially mineralized ones (mainly of the porphyry copper type) from 1225 to 2235 ppm. $\delta^{34}S(S^{2-})$ values of apatite, both from barren and mineralized intrusions, range from –1.99 to +1.79 per mil and are typical of magmatic sulfur. Temperatures of 560 to 840 °C deduced from the isotope fractionation between sulfide- and sulfate-derived sulfur in apatite ($\Delta^{34}SO_4^{2-}-S^{2-}$ ranging from 5.8 to 10.5 per mil) correspond to those calculated from $Fe^{2+}-Fe^{3+}-Mg^{2+}$ solid solution data of fresh primary biotite and biotite formed during potassic alteration. The absolute SO_4 content of apatite, rather than its oxidized / reduced sulfur ratio, may be taken to distinguish barren from mineralized intrusions for the investigated area. A cut-off value of ~ 1000 ppm can be defined as an exploration aid and indicator of potentially mineralized intrusions. This discrimination is consistent with that indicated by elevated X_{PDoxy} (proton deficient oxyannite) components in primary biotite and biotite formed during potassic alteration, and it confirms the need for elevated fO_2 ($> ~ 10^{-10}$) in the magma prior the separation of an aqueous, metal-charged fluid, for the subsequent formation of a mineral deposit. Weak propylitic alteration does not substantially affect the sulfur isotope equilibrium in apatite, whereas under such conditions major $Fe^{2+}-Fe^{3+}$ redistribution may occur in biotite and thus limits the applicability of biotite solid solutions to defining initial fO_2.

Combined apatite sulfur and biotite solution data enabled to delineate the evolutionary path of the mineralizing fluid in the porphyry copper syenite of Skouries (NE Chalkidiki pensinsula), representing a typical mineralized intrusion within the SMM.

Keywords: apatite, biotite, solid solution, porphyry copper, ore deposits, sulfur isotopes, oxygen fugacity, Serbomacedonian Massif, Greece.

Introduction

The importance of fO_2 levels, besides the prerequisite of elevated metal, chloride and sulfur contents in magmas, for the genesis of potentially mineralized intrusions, has been stressed in the past (JACOBS and PARRY, 1979; CHIVAS, 1981; MOORE and CZAMANSKE, 1973; CZAMANSKE and WONES, 1973; CREASY, 1966; NIELSEN, 1968; and others). Mg increases and Fe decreases in ferro-

[1] Present and correspondence address:
Gruppe Isotopengeologie, Mineralogisch-Petrographisches Institut, Universität Bern, Erlachstr. 9a, CH-3012 Bern, Switzerland. E-Mail: robert@mpi.unibe.ch.
Institut für Kristallographie und Petrographie, Laboratorium für Isotopengeologie, ETH-Zentrum, CH-8092 Zürich, Switzerland.

magnesian minerals from early to late magmatic and post-magmatic hydrothermal stages (CHIVAS, 1981; JACOBS and PARRY, 1979). Likewise JACOBS and PARRY (1979) showed that the Fe^{2+}/Fe^{3+} ratio in biotite increases progressively from igneous to secondary vein-biotite in the least altered and potassically altered parts of the Santa Rita porphyry (New Mexico). This trend is consistent with a decrease of fO_2 during late magmatic alteration and can be interpreted to result from fractional crystallization as the consequence of the partition between Fe and Mg. CHIVAS (1981) postulated that in a felsic magmatic system significant amounts of Na, K, Fe, Ti and Cl enter the coexisting fluid phase, whereas Si, Mg, Mn and Ca are preferentially retained in the silicate fraction. Elevated fO_2 conditions thus favour the ferric over the ferrous iron to coexist with magnesium in the melt and leads to the crystallization of Mg-enriched phases. Because the ratio $Mg/(Mg + \Delta Fe)$ is a measure of the degree of oxidation, the composition of biotites (in terms of $Fe^{2+}/Fe^{3+}/Mg^{2+}$) can be used to characterize oxygen fugacity (fO_2) trends in intrusions. It consequently allows to constrain the conditions under which separating fluids develop. However, based on the experiments of WONES and EUGSTER (1965), biotite solid solution data are only valid if biotite coexisted with K-feldspar and magnetite.

The behaviour of sulfur resembles that of chlorine in that it is partitioned into the aqueous phase (OHMOTO and RYE, 1979). This results in a lowering of of fH_2S in the system, both by passage of H_2S from the melt into the newly created and expanding aqueous phase and by the formation of SO_2 (vapour), to reach the partition equilibrium

$$SH^-(melt) + 5\ OH^-(melt) \rightleftarrows 3\ O^{2-}\ (melt) + SO_2\ (vapour) + 3\ H_2\ (vapour).$$

As temperature in the separated aqueous phase decreases during its generally upward transport through superjacent fracture systems, SO_2 hydrolyzes to produce H_2S and H_2SO_4 (HOLLAND, 1967). The resulting increase in fH_2S causes precipitation of sulfides from the metal-chloride complexes, and the corresponding increase in fH_2SO_4 causes precipitation of anhydrite, a common mineral in the higher temperature alteration assemblage of porphyry copper deposits. Since the diffusivity of H_2O and O_2 in silicate melts has been found to be very low compared to H_2 (CARMICHAEL et al., 1974), upon loss of the latter to the superadjacent wallrocks, an increase in fO_2 results. This explains why increasing fO_2 can be regarded as a function of the degree of fluid exsolution. High fO_2 should therefore potentially lead

to mineralized intrusions, if sufficient Cl, S and enough base metal (e.g. Cu) is present in the magma and if they are partitioned into the fluids.
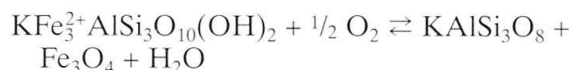
The following study aimed at testing the hypothesis of a close relationship between mineralizing trend and fO_2 in intrusions by a combined approach in which trace sulfur (SO_4^{2-}-derived / S^{2-}-derived sulfur concentration ratios) in apatite and bulk rock from barren and mineralized Tertiary intrusions within the Serbomacedonian Metallogenic Province (SMP) are compared with biotite solid solution data.

General considerations

Both oxidized and reduced sulfur may theoretically occur in apatite. Oxidized sulfur may substitute for phosphorus. Lattice-bound sulfur (as SO_4^{2-}) substitutes for phosphorus (PO_4^{2-}) and is present in the +VI oxidation state. The origin of reduced sulfur in apatite is more controversial. It is assumed that it mainly originates from hydrogen sulfide and its dissociation products (HS$^-$ and S^{2-}) in fluids that were trapped during crystal growth.

Biotite is a common constituent in many porphyry copper deposits. In such environments most biotites are igneous in origin or form during late-magmatic, potassic hydrothermal alteration. Because many thermodynamic variables control the chemistry of biotites, their compositions are potentially useful in understanding some of the physical and chemical conditions associated with the igneous and hydrothermal events leading to the formation of porphyry copper deposits. The compositions of ferromagnesian biotite may be represented by the end members $KMg_3^{2+}AlSi_3 O_{10}(OH)_2$ (phlogopite; phl), $KFe_3^{2+}AlSi_3O_{10} (OH)_2$ (annite; ann) and $KFe^{3+}AlSi_3O_{12}(H^{-1})$ (proton-deficient oxyannite; PDoxy). These end members form an additive ternary system in which three cations ($Mg^{2+}, Fe^{2+}, Fe^{3+}$) substitute in the trioctahedral lattice sites of the biotite structure. Substitution of Fe^{3+} is accompanied by loss of H^+ from the hydroxyl group in order to maintain electrical neutrality.

Activities of the annite component in ferromagnesian biotite solid solutions (EUGSTER and WONES, 1962), experimentally equilibrated with sanidine and magnetite by WONES and EUGSTER (1965) may be calculated from the equilibrium constant K for the reaction
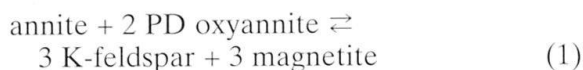
$$KFe_3^{2+}AlSi_3O_{10}(OH)_2 + \tfrac{1}{2}\ O_2 \rightleftarrows KAlSi_3O_8 + Fe_3O_4 + H_2O$$

at a given temperature and pressure, i.e. $K = f\ H_2O \times a_{sanidine} \times a_{mgt}/fO_2^{1/2} \times a_{ann}$, where

"f" denotes to the fugacity and "a" the activity of the subscribed species. Values of fH_2O at experimental temperatures and pressures are obtained from tabulated data of BURNHAM et al. (1969). Appropriate values of solid-solid buffer controlled fO_2 (WONES and EUGSTER, 1965) may be calculated using the following relationship (WONES, 1972):

$$\log fH_2O = 7409/T + 4.25 + \tfrac{1}{2}\log fO_2 + 3\log x - \log aKAlSi_3O_8 - \log aFe_3O_4,$$

an expression relating mole fraction Fe^{2+} x, temperature T, and the fugacities of oxygen (fO_2) and H_2O (fH_2O).

If biotite, K-feldspar and magnetite are in equilibrium with the fluid from which they crystallized, the following equation holds:

$$\text{annite} + 2 \text{ PD oxyannite} \rightleftarrows$$
$$3 \text{ K-feldspar} + 3 \text{ magnetite} \qquad (1)$$

The equilibrium constant of equation (1) reduces to $K = 1/a_{ann} \times a^2_{PDoxy}$, where a stands for activities of the two components in the biotite solid solution, and the activities of K-feldspar and magnetite are taken as unity for simplicity. Numerical expressions of activity coefficients for ann, PDoxy and phl as a function of each mole fraction based on thermodynamic analyses of ferromagnesian biotites can be computed after BEANE (1974) as follows:

$$\log K = -\log X_{ann} - 2\log X_{PDoxy} +$$
$$13.3\, X^2_{phl} + 27.6\, X^2_{PDoxy} + 55.5\, X^2_{ann}$$
$$-20.8\, X_{phl}X_{PDoxy} + 68.8\, X_{phl}X_{ann} \qquad (2)$$

Furthermore, the equilibrium constant of reaction (1) can be computed as a function of temperature:

$$\Delta G° = \Delta H° + T\Delta S° = -RT\ln K \qquad (3)$$

R denotes the gas constant (1.987 cal K^{-1} mol^{-1})

According to WONES and EUGSTER (1965), the effect of pressure variations on the compositions is small to negligible. By fixing X_{PDoxy} and iterating on X_{phl} until the right side of equation (2) is equivalent to the calculated value of $\log K$ at given temperatures (equation 3), it is possible to construct a series of equilibrium curves for the assemblage Fe-Mg-biotite + magnetite + sanidine as a function of temperature and X_{phl} at fixed values of X_{PDoxy} (as shown in Fig. 5).

Analytical techniques

Pure biotite concentrates (~ 20 mg) were obtained from crushed rock samples by magnetic and heavy liquid separation techniques and finally by handpicking. Fe^{2+} and Fe^{3+} were analyzed using the procedure described by AYRANCI (1977), which was correspondingly reduced to small sample amounts. The colorimetrical analyses were performed in 1 cm cells and the calibration of the ferrous and total iron was carried out with four independently processed biotite standards (MICA FE), whereas the stock solution of one (cross-checked by the three other standard samples) was used for the 5-point calibration curve. Mg was analyzed by flame-AAS, whereby the same stock solution as for the colorimetrical calibration served as calibration solution for the AAS also.

Powdered rock samples were pretreated in order to remove CO_2 mainly derived from carbonates which usually were present in minor amounts and complicated the sulfur gas separation. Therefore, an amount of 100 ml of 1M CH_2COOH (acetic acid) per 25 g of powdered sample was added and kept in an ultrasonic bath for 5 minutes. After one hour the suspension was filtered through an aspirator vacuum into a < 43 μm milipore filter, washed and dried in an oven at 60 °C over night.

The analyses of rock- and apatite sulfur basically followed the "Kiba"-technique (KIBA et al., 1955), which was optimized and modified by UEDA and SAKAI (1983). The extraction line used to separate sulfate and sulfide sulfur as SO_2 and H_2S, respectively, and carbonate carbon as CO_2, by successive vacuum destillation of a single aliquot of rock or mineral powder was constructed by A. Ueda at the Institute for Study of the Earth's Interior (I.S.E.I.), Okayama University, Misasa, Japan. Rock samples of 10 to 15 g and apatite samples of 1 to 2 g were dissolved in 200 to 220 g of "Kiba"-solution (dehydrated phosphoric acid with stannous ions as a reducing agent). Apatite reacted completely, whereas the bulk rock samples, specially magnetite and other resistent non-silicate phases, did not react fully. The extraction technique is described in detail by UEDA and SAKAI (1983). In the present work it has been applied to small quantities of apatite for the first time. A minimum of 0.0013 mmol SO_2 at STP (standard temperature and pressure) conditions was sufficient for the mass-spectrometrical analyses using the coldfinger technique. A blank value for H_2S-derived SO_2 of 273 pmol was calculated from an equally treated blank sample consisting of 200 g "Kiba"-solution. The amount of SO_2 from SO_4^{2-} was below the volumetrical detection limit.

The sulfur isotope analyses were performed on an automated SIRA 10 mass spectrometer at

I.S.E.I. The results are expressed in the usual delta notation as deviations in per mil of the $^{34}S/^{32}S$ ratio from that of the standard CDT (Canyon Diablo Troilite). As an internal laboratory standard, barium sulfate samples (MSS-3, MSS-2-2) were measured to control the reproducibility and to determine the fractionation factor. From four analyses of the MSS-3 and MSS-2-2 reference samples $\delta^{34}S_{CDT}$ values of 3.50 ± 0.01 and 21.56 ± 0.12 per mil were obtained. These values, within the assigned errors, are within the range of long term reference sample measurements monitored at I.S.E.I. (3.5 ± 0.1 and 21.5 ± 0.1 per mil, respectively). Oxygen isotope effects on the sulfur isotope ratio measurements are summarized in FREI (1992). $\delta^{34}S$ values and concentrations of sulfate were corrected according to UEDA and SAKAI (1983), taking into account the reduction of the small fraction of sulfate to H_2S during the "Kiba"-technique even under vacuum.

Geological frame

A variety of mineral deposits occur within the Serbomacedonian Massif (SMM). They are genetically related to Tertiary intrusions which were emplaced during a period of extensional tectonics. Some of the mineralizations are of economic interest and form potential ore deposits in former Yugoslavia, Bulgaria and Northern Greece. A large NW–SE trending belt between Belgrade (Croatia) and the Chalkidiki peninsula (Greece), which JANKOVIC (1977, 1978) defined as the Serbomacedonian Metallogenic Province (SMP), comprises mineralizations of a specific elemental association, mainly Pb, Zn, Sb, Bi, Mo, Cu, Fe, Sn, Au, Ag, Sb, Hg and U. The intrusions occur in a belt crossing the main NNW–SSE tectonic lineament of the SMM at an angle of ~ 15° in a NW–SE direction. The variety of mineralizations within this zone ranges from Pb–Zn replacements, fracture controlled vein-type occurrences, SEDEX-type deposits and porphyry copper type mineralizations (NEUBAUER, 1956, 1957; NICOLAOU, 1960, 1964, 1969; KOCKEL et al., 1975; PAPADAKIS, 1975); KALOGEROPOULOS et al. (1989); FREI (1992); GILG (1993); GILG and FREI (1993); FREI (1995); FREI and GILG (in prep.). In northern Greece two main areas of intrusive activity can be distinguished (TOMPOULOGLOU, 1989; FREI, 1992), one is located in the northwestern and the other in the southeastern part of the SMM (Fig. 1). The compositional trend is (monzo)diorite – granodiorite – granite, whereas smaller stocks and dikes show latitic, trachytic and andesititc compositions. They represent members of a typical calc-alkaline suite emplaced during the time between middle Eocene and middle to late Miocene (KOCKEL et al., 1975; FREI, 1992; GILG, 1993; GILG and FREI, 1994; PAPADAKIS, 1972; TOMPOULOGLOU, 1989; DE WET and MILLER, 1987; CHRISTOFIDES et al., 1990). Three groups can be distinguished:

1. Mineralized (porphyry copper-type) intrusions with well developed alteration halos (Fisoka diorite porphyry complex, Jerakario syenite porphyry) and others with only a narrow alteration zone (e.g. Skouries syenite porphyry). Mineralization is either restricted to veins and/or occurs in disseminated form, and mainly consists of pyrite, chalcopyrite, bornite, and gold.

2. Unmineralized intrusions with extensive phyllic alteration halos developed in the country rocks (e.g. [monzo]diorite complex of Tsikara-Vathilakkos-Asproloakkos).

3. Barren intrusions without alteration halos, partly related in space to mineralized stocks (Jerissos granite, Stratoni granodiorite, trachytic to andesitic stocks and dikes in the Asprolakkos and Stratoni area).

A summary of the mineralogical and petrographical properties of the intrusions is given in table 1.

The SMM is considered to represent a Paleozoic or older basement complex on the Balcan Peninsula. In Northern Greece it consists mainly of three geotectonic units, i.e. the widespread Vertiskos- and the Kerdyllia Units, and intercalated series pertaining to the Circum Rhodope Belt (CRB). The majority of the investigated Tertiary intrusions are emplaced in the Vertiskos Unit, except for the Stratoni granodiorite (ASPCHO-1, ST-11), the Stratoni monzodiorite (ST-1A), and the porphyritic andesite dike (ML-4) from Madem Lakkos which occur within the Kerdyllia Unit (Fig. 1). The latter comprises mainly biotite gneisses, hornblende-biotite gneisses and amphibolites as well as distinct marble horizons. The Kerdyllia Unit has been metamorphosed under upper amphibolite facies metamorphic conditions and locally incipient anatectic features have been observed (DIXON and DIMITRIADIS, 1984; SAKELLARIOU, 1989). The Vertiskos Unit is in tectonic contact with the Kerdyllia Unit. Two-mica gneisses and schists with intercalated biotite- and biotite-hornblende gneisses as well as amphibolites are the most prominent lithologies. They are metamorphosed in the lower amphibolite facies. Retrograde mineral assemblages are common in the gneisses and schists and point to a later (Paleozoic or Alpidic) thermal event. Neotectonic and seismic activities in the SMM are still very widespread (PAVLIDES et
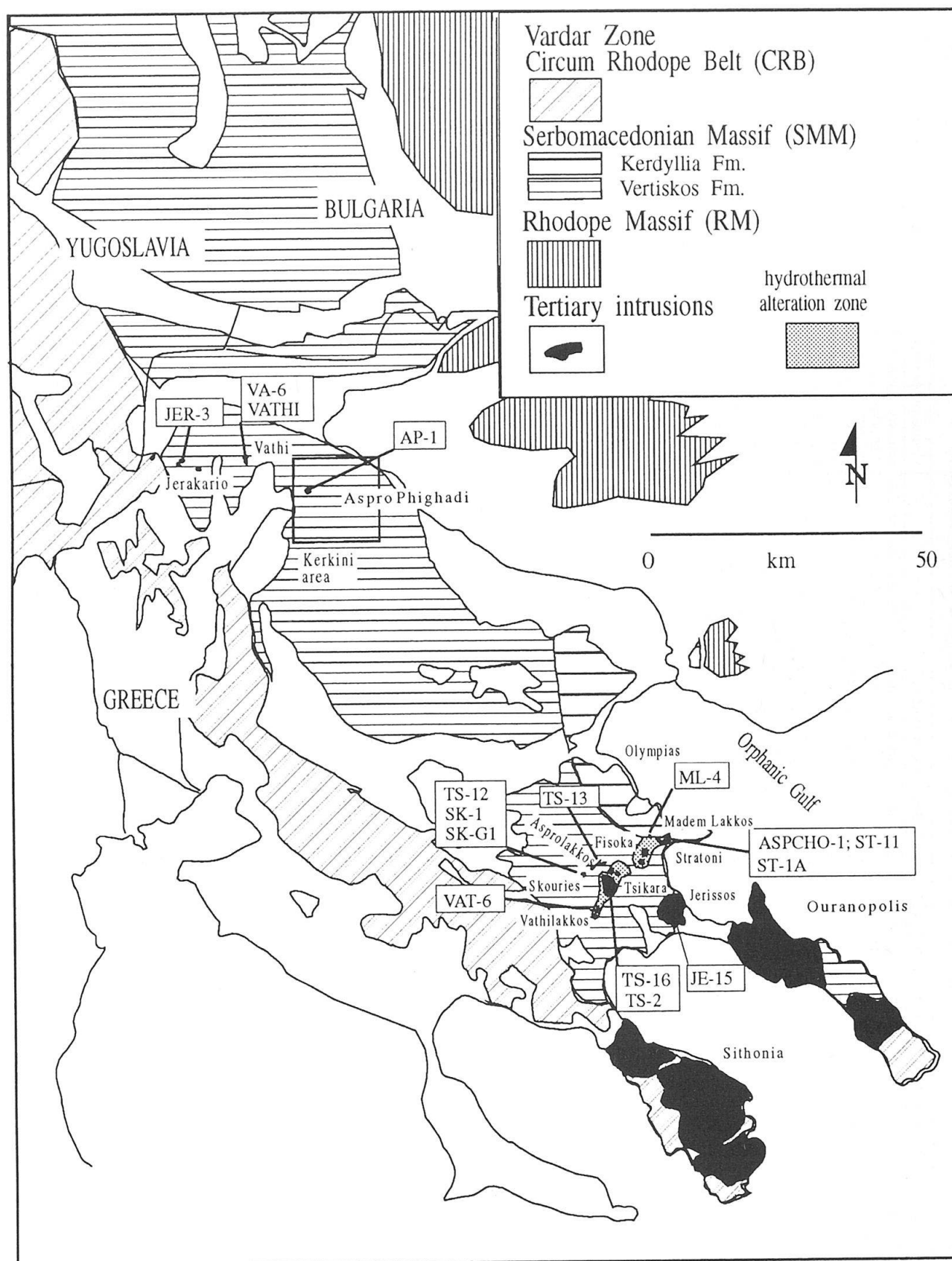
Fig. 1 Simplified geological map of the Serbomacedonian Massif (SMM) of Northern Greece with sample locations (square boxes with sample names). The location of main ore deposits related to Tertiary intrusions, i.e. Au-bearing, carbonate-hosted Pb–Zn deposits (Madem Lakkos, Olympias) and vein-type Cu–Pb–Zn–As occurrences (Kerkini area) are also indicated.

Tab. 1 Summary of the mineralogical properties and the intrusion ages of the investigated Tertiary intrusions.

location	sample	intrusive type	group	mineralization	alteration	mineralogy	biotite properties	age (Ma)	data	references
Jerakario	JER-3	porphyritic syenite	1	porphyry copper	potassic ± propylitic	plag, kfs, qtz, bio, ± hbl as phenocrysts, matrix of pink kfs, qtz, diss. mag	primary, idiomorphic bio, secondary bio ± chloritized	22 ± 6	1, 2, 3	1, 2
Vathi	VA-6	quartz-monzonite	1	porphyry copper	partly potassic	plag, kfs, hbl, bio, qtz, diss. mag	primary, idiomorphic bio, secondary bio in veinlets with kfs, py, stb	18 ± 2	1, 2, 3	1, 2, 3
Vathi	VATHI	quartz-monzonite	1	porphyry copper	partly potassic	equigranular plag, kfs, hbl, bio, ± qtz, diss. mag	primary, idiomorphic bio	17 ± 2	2, 3	1, 2, 3
Aspro Phighadi	AP-1	porphyritc latite	3	porphyry copper?	weakly propylitic	plag, kfs, hbl and bio as phenocrysts, finegrained matrix of kfs, qtz, mag, tit	primary, idiomorphic bio, chloritized, secondary bio replaces hbl	–	2	1, 2
Stratoni	ASPCHO-1	granodiorite	3	barren	weakly propylitic	equigranular plag, kfs, qtz, bio, ± hbl, minor py, chl, epi as secondary phases	primary, idiomorphic bio, chloritized	27.9 ± 1.2	1, 2, 3	2, 4, 5, 6
Stratoni	ST-1A	(monzo-) diorite	3	barren	weakly propylitic	coarse grained ploag, cpx, hbl, ± kfs, diss. mag, minor py, chl, secondary epi	primary, idiomorphic bio, chloritized	26.9 ± 2.0	1, 2, 3	2, 5, 6
Stratoni	St-11	granodiorite	3	barren	weakly propylitic	medium grained plag, kfs, qtz, bio, diss. mag, epi, chl, secondary py	primary bio, flow textured, chloritize	–	1	2
Stratoni	ML-4	porphyritic andesite	3	barren	unaltered	plag, hbl, bio as phenocrysts, aphanitic matrix with kfs and diss. mag	primary bio, flow textured	19.1 ± 0.6	2	2, 5, 6
Tsikara-Asprolakkos	TS-2	porphyritic andesite	2	barren	weakly propylitic	plag, hbl, bio and cpx as phenocrysts, matrix of plag, kfs, diss. mag	primary, idiomorphic bio, chloritized	–	2	1, 2, 7
Tsikara-Asprolakkos	TS-16	monzodiorite	3	barren	weakly propylitic	hypidiomorphic texture, finegrained plag, kfs, cpx, hbl, ± qtz, diss. mag	primary, idiomorphic bio, chloritized	27.5 ± 0.4	2	2, 7
Tsikara-Asprolakkos	TS-13	porphyritic latite	3	barren	weakly propylitic	plag, kfs, bio, hbl as phenocrysts, matrix of same mineralogy, ± qtz, diss. mag	primary, idiomorphic and flow textured bio, chloritized	–	1	2
Tsikara-Vathilakkos	VAT-6	monzodiorite	2	barren	weakly propylitic	equigranular plag, kfs, hbl, bio, ± cpx, diss. mag, ± py	primary, idiomorphic bio, choritized	–	2	2
Jerissos	JE-15	granite	3	barren		weakly propylitic	primary, idiomorphic bio, ± chloritized	54.3 ± 0.3	1, 2, 3	2
Skouries	TS-12	porphyritic trachyte	3	barren	unaltered	porphyritic texture, plag, kfs, primary bio, ± qtz, ± hbl, finegrained matrix with diss. mag	idiomorphic, partly flow-textured brown bio		1, 2, 3	2, 8
Skouries	SK-1	porphyritic syenite	1	porphyry copper	potassic	porphyritic texture, plag, kfs, bio ± qtz, ± hbl, pink kfs, ± qtz, secondary biotite, stringy mag in finegrained matrix	finegrained secondary bio		1	2, 8
Skouries	SK-G1	porphyritic syenite	1	porphyry copper	potassic, propylitic	porphyritic texture, as in SK-1, with patchy chloritization of hbl, py and cc in matrix, diss. py and cpy	primary bio, secondary bio chloritized	19 ± 2	1, 2, 3	2, 8

bio = biotite; plag = plagioclase; kfs = K-feldspar; hbl = hornblende; cpx = clinopyroxene; qtz = quartz; chl = chlorite; epi = epidote; tit = titanite, mag = magnetite; py = pyrite, cc = calcite; cpy = chalcopyrite, stb = stibnite; diss = disseminated; data: 1 = biotite solid solution; 2 = bulk rock sulfur; 3 = apatite sulfur; group: numbers refer to those in table 1. References: 1 = TOMPOULOGLOU (1981); 2 = FREI (1992); 3 = FILIPIDES et al. (1988); 4 = KALOGEROPOULOS et al. (1981); 5 = GILG and FREI (1994); 6 = GILG (1993); 7 = KOCKEL et al. (1975); 8 = FREI (1995).

Tab. 2 Average compositions of biotites from barren and mineralized intrusions of the SMM with calculated equilibrium temperatures and oxygen fugacities

sample	intrusive type	group	Fe^{2+} (wt%)	Fe^{3+} (wt%)	Mg^{2+} (wt%)	X_{ann}	X_{phl}	X_{PDoxy}	n	fO_2	T (°C)
				barren intrusions							
ASPCHO-1	granodiorite	3	11.18	0.64	8.75	0.54	0.43	0.03	2	$< 10^{-35}$	206
ST-11	granodiorite	3	10.65	2.50	8.63	0.49	0.40	0.11	3	$\sim 10^{-29}$	359
ST-1A	(monzo)diorite	3	9.99	1.89	8.26	0.50	0.41	0.09	3	$\sim 10^{-33}$	324
TS-13	porphyritic latite	3	10.53	1.68	8.19	0.51	0.41	0.08	3	$\sim 10^{-34}$	291
VAT-6	monzodiorite	2	9.35	0.84	9.48	0.48	0.48	0.04	5	$< 10^{-35}$	274
JE-15	granite	3	13.13	0.55	6.84	0.64	0.33	0.03	4	$< 10^{-35}$	147
				porphyry copper							
JER-3	porphyritic syenite	1	7.52	5.69	7.63	0.36	0.37	0.27	3	$\sim 10^{-8}$	888
VA-6	quartz-monzonite	1	7.62	4.75	8.76	0.37	0.41	0.22	2	$\sim 10^{-10}$	780
				Skouries porphyry copper							
TS-12	porphyritic trachyte	3	5.12	3.38	11.16	0.26	0.57	0.17	3	$\sim 10^{-10}$	939
SK-1	porphyritic syenite	1	5.60	2.68	11.39	0.28	0.58	0.14	6	$\sim 10^{-13}$	750
SK-G1	porphyritic syenite	1	6.67	1.62	10.87	0.35	0.57	0.08	4	$\sim 10^{-22}$	487

The mole fractions are calculated assuming that all trioctahedral lattice sites are occupied by either Fe^{2+}, Fe^{3+} or Mg^{2+}.
Temperatures calculated according to equation (3). The analytical error of the concentration measurements (AAS and colorimeter) is in the order of $\sim \pm 2\%$, inducing an uncertainty in the calculated temperatures of $\sim \pm 5\%$. n = number of independant analyses.
ann = annite; phl = phlogopite; PDoxy = proton-deficient oxyannite; group numbers refer to those in table 1.

al., 1991; VOIDOMATIS et al., 1990; KONDOPOULOU and WESTPHAL, 1986). Various attempts were undertaken to relate the magmatic activity and associated metallogeny in this province to plate tectonic developments in the northeastern Mediterranean (PAPADOPOULOS and and ANDINOPOULOS, 1984; FYTIKAS et al., 1980; CHANNELL and HORVATH, 1976; DEWEY et al., 1973). Their models prefer a contemporaneous metallization in this belt. The coexistence of barren and mineralized (porphyry copper-type) intrusions and their commonly close spatial relation to economically important polymetallic sulfide deposits (e.g. Madem Lakkos, Olympias) and vein-type Pb–Zn–Mn occurrences (e.g. Kerkini area) makes the northern Greek SMM an ideal study area for metallogenic processes related to magmatic rocks.

Results

BIOTITE SOLID SOLUTIONS

Biotite in mineralized (porphyry copper type) intrusions is characterized by elevated X_{PDoxy} (~ 0.15) and higher Mg^{2+}/Fe^{2+} ratios (> 0.5) rela-

tive to biotite from barren intrusions ($< \sim 0.11$ and > 0.5, respectively). Furthermore, $Mg/(Mg + Fe_{tot})$ ratios (by weight) of all biotites are < 0.47, a value which has been proposed by KESLER et al. (1975) for the discrimination of igneous from hydrothermal biotite. This discrimination is compatible with investigations by MOORE and CZAMANSKE (1973), JACOBS and PARRY (1979), CREASY (1966), FOURNIER (1967) and NIELSEN (1968), who showed that alteration biotite in porphyry copper deposits exhibit higher molecular ratios of Mg:Fe than earlier igneous biotite. Microscopic observations reveal unequivocally that in all samples primary biotite, – and in the case of the porphyry copper intrusions, biotite formed during potassic alteration – coexists with K-feldspar and disseminated magnetite. Therefore the WONES and EUGSTER (1965) approach to calculate approximative equilibrium temperatures and consequently to deduce oxygen fugacity levels on the basis of biotite solid solution data is justified. Oxygen fugacities were graphically estimated from the JACOBS and PARRY (1979) logfO_2 vs T graph (their Fig. 10). Activities of magnetite and K-feldspar were taken as unity for simplicity. Data are listed in table 2, wherby the relative approximate positions to the Ni–NiO and hematite-
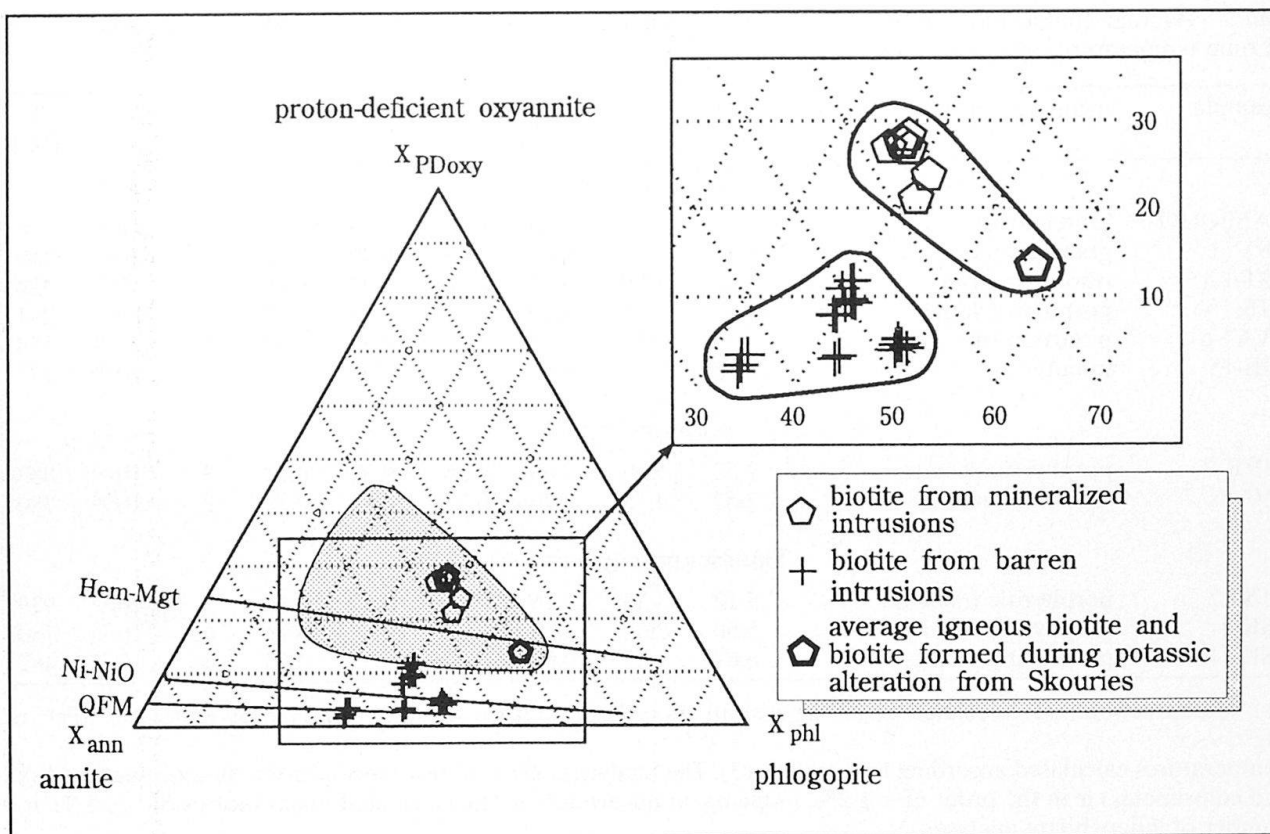
Fig. 2 Ternary diagram with biotite compositions from mineralized and barren intrusions in the SMM (adapted from JACOBS and PARRY, 1979). The composition of biotite from the Skouries porphyry copper intrusion is indicated as an average value of primary and secondary biotite. The field of "igneous" biotite (shaded area) summarizes data from HEINRICH (1946) and FOSTER (1960).

magnetite buffer lines in this graph were estimated by their corresponding plot position in the triangular diagram in figure 2 (adapted from JACOBS and PARRY, 1979). A maximum error from this graphic approach is estimated to be ~ ± 2 log units fO_2.

Biotite from barren intrusions in the SMM plot below the field of igneous biotite (outlined in Fig. 2) published by FOSTER (1960) and HEINRICH (1946). The results indicate that during the formation of biotite in barren intrusions the mean oxygen fugacity was below or slightly above the Ni–NiO buffer. Biotite from the barren Jerissos granite yielded the highest X_{ann} and the lowest X_{PDoxy}. Biotite compositions from the mineralized, porphyry copper type intrusions scatter around the magnetite-hematite oxide buffer line. Among these, biotite from Skouries is characterized by the highest X_{phl} components. Equilibrium temperatures are correspondingly higher in the mineralized (range from 490 to 940 °C) compared to the barren intrusions (range from 150 to 360 °C). The temperature ranges are consistent with those proposed by HUNT (1991), i.e. 600–

900 °C for intrusive to late magmatic stages of porphyries and 200–350 °C for late stage alteration processes, respectively.

Graphically estimated fO_2 values for biotite from the barren intrusions are very low ($< \sim 10^{-29}$) and therefore do not indicate significant oxidizing conditions during their formation. These low values result from redistribution processes during near-surface conditions, as fO_2-values $< 10^{-35}$ imply fH_2O values $< \sim 20$ bars and thus $P_{H_2O} < \sim 0.1$ kbar (BURNHAM et al., 1969). Igneous biotite or biotite formed during potassic alteration in the mineralized porphyries, however, indicate elevated fO_2 conditions during their crystallization ($> 10^{-13}$).

SO_4^{2-}-DERIVED AND S^{2-}-DERIVED SULFUR ANALYSES

Table 3 lists the sulfur concentrations and sulfur isotope ratios of bulk rock and apatite from barren and mineralized intrusions in the SMM. The significance of data from the Skouries porphyry

Tab. 3 Sulfur concentrations and sulfur isotope ratios of bulk rock and apatite from barren and mineralized intrusions in the SMM.

sample	rock type	group	S (S²⁻) (ppm)	S(SO₄²⁻) (ppm)	S_tot (ppm)	δ³⁴S(S²⁻)	δ³⁴S (SO₄²⁻)	δ³⁴S_(tot)	Δ³⁴S (S²⁻-SO₄²⁻)	T (°C) ± 2σ	S(SO₄²⁻) S(S²⁻)
					bulk rocks (barren intrusions)						
ST-1A	(monzo)diorite	3	136.1	41.9	178.0	−0.44	+2.74	+0.31	3.18	1209 ± 52	0.31
ASPCHO-1	granodiorite	3	149.9	21.2	171.1	−4.70	−0.57	−4.19	4.13	1036 ± 36	0.14
JE-15	granite	3	8.1	3.1	11.2	+0.04	+6.55	+1.84	6.51	778 ± 18	0.38
AP-1	porphyritic latite	3	3.3	6.9	10.2	+2.33	+7.84	+6.06	5.51	866 ± 24	2.09
TS-2	porphyritic andesite	2	39.7	19.2	51.9	−6.51	+1.93	−4.27	8.44	653 ± 12	0.48
TS-16	monzodiorite	3	67.9	8.2	76.1	−3.27	+0.05	−2.91	3.32	1179 ± 48	0.12
VAT-6	monzodiorite	2	26.5	74.6	100.9	−4.39	+8.67	+5.26	12.99	476 ± 6	2.82
ML-4	porphyritic andesite	3	46.1	52.3	98.4	−4.83	+4.61	+0.19	9.44	604 ± 10	1.13
TS-12	porphyritic trachyte	3	13.4	63.7	78.1	−1.26	+5.55	+4.31	6.81	755 ± 18	4.75
					bulk rocks (mineralized intrusions)						
SK-G1	porphyritic syenite	1	130.8	49.6	180.4	−1.81	+4.15	-0.17	5.96	824 ± 22	0.98
JER-3	porphyritic syenite	1	3.4	319.3	322.7	−1.37	+4.23	+4.17	5.60	858 ± 24	94
VA-6	monzonite	1	20.5	5.5	26.0	−0.83	+3.73	+0.13	4.56	975 ±3 0	0.17
VATHI	monzonite	1	4.2	15.6	19.8	+2.53	+6.86	+5.94	4.33	1007 ± 34	3.71
					apatites (barren intrusions)						
ST-1A	granodiorite	3	15.2	570	575.2	−1.99	+8.48	+8.20	10.47	560 ± 9	37.5
ASPCHO-1	granodiorite	3	27.1	402	429.1	+0.37	+8.03	+7.54	7.66	698 ± 15	14.8
JE-15	granite	3	5.2	575	580.2	+0.98	+8.29	+8.23	7.31	720 ± 16	110
TS-12	porphyritic trachyte	3	75.1	1791	1866.4	+1.79	+8.49	+8.22	6.70	763 ± 18	23.8
					apatites (mineralized intrusions)						
SK-G1	porphyritic syenite	1	51.2	1324	1375.2	−1.97	+6.41	+6.10	8.39	656 ± 13	25.9
JER-3	porphyritic syenite	1	296.6	2037	2233.6	+0.74	+6.57	+6.09	5.83	836 ± 21	6.9
VA-6	monzonite	2	10.9	1214	1224.9	−0.53	+7.24	+7.17	7.77	691 ± 14	111
VATHI	monzonite	2	12.2	1521	1533.2	+1.71	+7.57	+7.52	5.86	833 ± 21	125

δ-values are given as per mil deviations between the sample and the Canyon Diablo Troilite (CDT) sulfur standard. $\Delta \sim 1000 \times \ln\alpha_{\text{sulfate-sulfide}} = 7.4 \times 10^{6}/T^{2} -0.19$ (MIYOSHI et al., 1984). Errors calculated on the basis of a 0.12 per mil absolute reproducibility (2σ) of the MSS-2-2 barium sulfate reference sample assigned to the individual sulfur isotope analyses. Group numbers refer to those in table 1.

copper area are discussed in detail in the respective chapter.

Barren intrusions are characterized by bulk rock oxidized and reduced sulfur concentrations in the range of 3.1–74.6 ppm and 3.3–149.9 ppm. Sulfur concentrations in apatite from barren intrusions show a narrower spread. SO_4^{2-}-derived sulfur varies between 402–570 ppm, whereas S^{2-}-derived sulfur is in the range of 5.2–27.1 ppm. $\Delta^{34}S$-values of both apatite sulfur components are relatively homogeneous (range from −1.99 to +1.79 per mil for S^{2-}-derived, and from +8.01 to +8.49 per mil for SO_4^{2-}-derived sulfur), whereas they show a wider spread in the bulk rock analyses (range from −6.51 to +2.33 per mil and from −0.57 to +8.67 per mil, respectively).

The mineralized intrusions have S^{2-} and SO_4^{2-}-derived sulfur concentrations varying be-

tween 3.4 and 130.8 ppm and between 5.5 and 319.3 ppm, respectively. S^{2-}-derived sulfur concentrations in apatite vary from 10.9–296.6 ppm whereas SO_4^{2-}-derived sulfur ranges from 1214–2037 ppm. In bulk rock the corresponding $\delta^{34}S$-values range from −6.51 to +2.33 and from −0.57 to +8.67 per mil, respectively. Apatite is characterized by $\delta^{34}S(S^{2-})$-values ranging from −1.97 to +1.71 and by $\delta^{34}S(SO_4^{2-})$ values from +6.41 to +7.57 per mil.

SO_4^{2-}-derived/S^{2-}-derived sulfur ratios are highly variable for bulk rock and apatite. An expected systematic trend towards elevated ratios in bulk rock and/or in apatite from mineralized intrusions relative to barren ones cannot be delineated. The variability of $\Delta\delta^{34}S$-values is greatest in bulk rock from barren intrusions, whereas it is relatively uniform in apatite from mineralized

intrusions. Temperatures, calculated on the basis of the experimental fractionation factor between sulfate and sulfide in a alkali-chloride melt (MI-YOSHI et al., 1984), reflect the variability of sulfur isotope data, in that they are generally more consistent in apatite than those from bulk rock and reflect magmatic to late magmatic-hydrothermal conditions. Bulk rock sulfur isotope equilibrium seems to be highly sensitive to even weak post-magmatic alteration processes and therefore the calculation of equilibrium temperatures does not lead to geologically meaningful values.

Discussion

The sulfur concentrations, and correspondingly the SO_4^{2-}-derived/S^{2-}-derived sulfur ratios of bulk rock from barren and mineralized intrusions in the SMM, do not discriminate between the two types of intrusions. Elevated S^{2-}-derived sulfur concentrations in barren intrusions (samples ST-1A, ASPCHO-1 and TS-16) might reflect the presence of minor pyrite formed during weak propylitic alteration. The high sensitivity of the SO_4^{2-}-derived/S^{2-}-derived sulfur ratios of bulk rock towards even weak alteration processes limits the use of bulk rock sulfur component analyses to discriminating potentially mineralized from initially barren intrusions. Very low (~ 10 ppm S_{tot}) sulfur contents occur in the barren granite of Jerissos (JE-15) and the porphyritic latite of Aspro Phighadi (AP-1). They are characterized by opposing SO_4^{2-}-derived/S^{2-}-derived sulfur ratios. A predominance of SO_4^{2-}-derived over S^{2-}-derived sulfur is characteristic of the latite porphyry, whereas the proportions are reversed for the granite. This either indicates that more oxidizing conditions prevailed in the latitic- compared to the granitic melt or else it could reflect the incorporation of a foreign, heavy sulfate-sulfur from parental (sedimentary?) rocks of the Vertiskos Formation into the latitic melt during its generation. Sulfur isotope analyses, performed on both sulfur components, constrain these possibilities. The similar $\Delta^{34}S(SO_4^{2-})$ values, i.e. +6.55 and +7.84 per mil of the granite and the latite porphyry, conform with the overall range of +6.41 to +8.49 per mil for apatite and thus with values typical of magmatic oxidized sulfur (Tab. 3). Therefore sulfate contamination of the latitic magma is highly improbable to explain the the predominance of oxidized over reduced sulfur in the latite. The $\Delta^{34}S_{tot}$-values (+1.8 per mil for the granite and +6.0 per mil for the latite) may simply reflect a combination of higher fO_2 and a lower equilibrium temperature in the latite com-

pared to the granite. This example demonstrates that a combination of concentration- and isotope data of both sulfur components can help to elucidate the origin of trace sulfur in intrusions. The range of –4.2 to +6.0 per mil for bulk rock $\Delta^{34}S_{tot}$-values is approximately compatible with the range –3 to +3 per mil for acidic igneous rocks and therefore with a magmatic source of the trace sulfur (OHMOTO and RYE, 1979). From the bulk rock sulfur isotope data alone it is however not possible to distinguish between magmas formed by partial melting of average crustal rocks and magmas formed by partial melting of mantle rocks, as their $\Delta^{34}S_{tot}$ values are essentially identical (OHMOTO and RYE, 1979).

Biotite solid solutions are easily affected by low temperature alteration, as calculated equilibrium temperatures (in the system bio – kfs – mgt – H_2O/O_2) in the barren intrusions are consistently too low to represent geologically meaningful formation temperatures. Postformational redistribution mainly of Fe^{2+} and Fe^{3+} is the cause for the deficency of X_{PDoxy} in the barren intrusions and is assumed to accompany weak propylitic alteration. Effects of the latter, i.e. slight chloritization of biotite edges, could be observed in all barren samples. As a consequence the calculated equilibrium temperatures at the best indicate a maximum temperatures at which iron redistribution occurred in biotite.

Apatite has been shown to be relatively inert towards post-magmatic alteration processes as it seems to retain sulfur isotope equilibrium and therefore yields geologically reasonable formation temperatures. This is in accordance with findings by BANKS (1982), who showed that the abundance of S in igneous apatite is not related to the amount of alteration of bulk intrusive samples from the Ray porphyry copper district (Arizona). S^{2-}-derived sulfur concentrations can be correlated with the microscopic observation that apatite contains fluid inclusions, in which it is assumed that reduced sulfur is present in a dissolved form as S^{2-} or HS^-. Furthermore, such inclusions are more common in apatite from mineralized intrusions than in apatite from barren intrusions and are also characterized by the occurrence of at least one highly birefrigent daughter phase, possibly a sulfate. Most of the reduced, and probably part of the oxidized sulfur in apatite therefore is suggested to be contained in these inclusion fluids. Generally the total sulfur concentrations of apatite correspond with the range of 100–500 ppm reported by BANKS (1982) for apatite from barren I-type granitoids in Southwestern North America. Apatite seems to preferentially fractionate oxidized sulfur from the melt
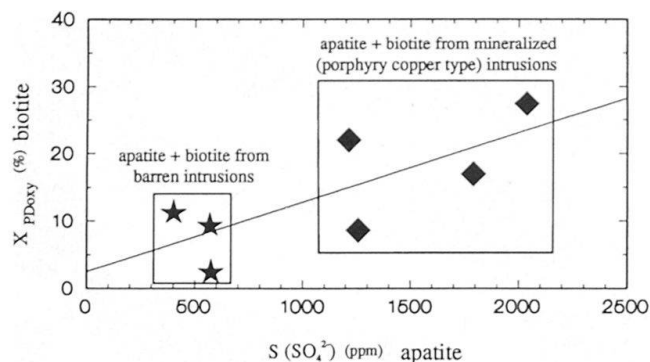
Fig. 3 X_{PDoxy} vs $S(SO_4^{2-})$ diagram depicting biotite and apatite data from mineralized and barren intrusions in the SMM. Mineralized trends in intrusions are indicated by elevated $S(SO_4^{2-})$ concentrations in apatite and higher X_{PDoxy} components in biotite from corresponding samples. A value of > = 1000 ppm of oxidized sulfur in apatite can be taken as an indicator for mineralizing trends.

into its lattice. Even in the granite of Jerissos (JE-15), in which the sulfur concentration is very low (11 ppm), sulfur within apatite is enriched by a factor of ~ 50 (Tab. 3). Igneous apatite can therefore be used as a primary "magmatic" sulfur indicator. Furthermore, an elevated (1260–2040 ppm) concentration of oxidized sulfur in this mineral is typical of mineralized (porphyry copper type) intrusions in this belt. Ultimately it is therefore supposed that the initial concentration of sulfur in the melt and the fO_2 level control the incorporation of SO_4^{2-} in apatites. The elevated SO_4^{2-}-derived sulfur concentration in apatite from mineralized intrusions corresponds well to elevated X_{PDoxy} components in primary biotite and biotite formed during potassic alteration. The following plot (Fig. 3) displays the positive relation between X_{PDoxy} components in biotite and oxidized sulfur concentrations in apatite from barren and mineralized intrusions in the SMM.

Provided that a melt is initially enriched in sulfur, S_{tot}, or even more pronounced, SO_4^{2-}-derived sulfur concentrations in apatite can be taken as an indicator for mineralized intrusions. A value over 1000 ppm may therefore be characteristic of a potentially mineralized intrusive rock in the SMM.

Case study: The Skouries porphyry copper deposit

The Skouries porphyry copper deposit was rediscovered in 1972 (ZACHOS, 1972). Archeological findings indicated that mining activity took place in this area as early as the 5th to 4th century

B.C. The economic interest in this deposit ended some ten years ago because of insufficient ore reserves and poor grade. However, due to recent new findings of elevated platinum-group elemental concentrations, mainly of Pd, Pt and Ru (ELIOPOULOS and ECONOMOU, 1991), this deposit, at least from a scientific view, became interesting again. In the latest publication, FREI (1995) has traced the evolutionary path of the mineralizing fluid in the porphyry copper system of Skouries using a combined radiogenic and stable isotope approach. The porphyritic syenite of Skouries intruded the Vertiskos Fm. of the SMM 19 Ma ago (FREI, 1992). Its location is marked on the map in figure 1. Based on i) their similar major and trace element concentrations, ii) their similar Pb and Sr isotope characteristics (FREI, 1995), and iii) their close spatial occurrence in the field, the porphyritic trachyte dike (sample TS-12) in the Asprolakkos area and the main, mineralized porphyritic syenite stock at Skouries (SK-1; SK-G1) are assumed to be cogenetic and contemporaneous. The aim is to show the significance and interpretation of sulfur and biotite solution data in the light of the established model for the evolution of the mineralizing fluid at Skouries:

Following its emplacement (stage I), the porphyritic syenite suffered a pervasive potassic alteration at temperatures of ~ 590 to 640 °C (stage II). Two subsequent veining stages with propylitic characteristics (stage IIIA at ~ 480 °C; stage IIIB at ~ 380 °C) brought most of the Cu, which was deposited in form of chalcopyrite. The range of $\delta^{18}O$ from +3.5 to +7.6 per mil (FREI, 1995) for the fluid in equilibrium with vein quartz point to typical ore forming fluids associated with porphyries. They represent magmatic fluids which may, to some extent, have interacted with the igneous wall rock. A subsequent late propylitic alteration (stage IV at ~ 210 °C), more localized and patchy, affected the country rocks and the porphyritic syenite and deposited disseminated pyrite and chalcopyrite. Pb isotopes indicate an evolution of the fluid composition from one characterized by magmatic components to one dominated by the country rocks. Fluids in veins within the porphyry could ascend rapidly from deeper levels without reacting with the host porphyry but picked up their Sr isotope signature from the country rocks.

In this example three of the above characterized evolutionary stages are represented by the following samples:
– Stage I by the unaltered porphyritic trachyte (TS-12)
– Stage II by the potassically altered porphyritic syenite (SK-1)

– Stage IV by the propylitically overprinted porphyritic syenite (SK-G1)

Results

Bulk rock sulfur concentrations (Tab. 3) in the trachyte indicate that initially the magma was low in sulfur (TS-12; S_{tot} ~ 80 ppm), whereas a significant amount of mainly reduced sulfur was added during stage IV (SK-G1; S_{tot} ~ 180 ppm). During this alteration the concentration of oxidized sulfur (~ 50 ppm) remained constant. This trend is consistent with the observation of disseminated sulfides in the patchy chloritized parts of the porphyry, and specifically in sample SK-G1. A drop in the $\delta^{34}S_{tot}$ values from +4.31 to –0.17 is assumed to indicate the change from initially oxidizing to more reducing conditions during late stage alteration at Skouries. The $\delta^{34}S$ value of bulk reduced sulfur in sample SK-G1 (–1.81 per mil) is consistent with $\delta^{34}S$ values of –0.23 and –2.14 per mil for disseminated pyrite and chalcopyrite in this sample (FREI, 1995) and therefore underlines the accurracy of the KIBA bulk rock analysis, which in this case was dominated by sulfide sulfur. The similarity between the isotope compositions of the sulfur components in both samples argues against a significant incorporation of heavy sulfur from the enclosing Vertiskos metasediments by interaction with the late stage IV propylitic fluids. This is in contrast to the results obtained from Pb isotopes which indicate a significant contamination of the propylitic fluid by Pb from the intruded country-rock. Comparison of sulfur isotope data from apatite with those from the corresponding bulk rocks TS-12 and SK-G1 suggests the presence of other sulfate bearing minerals with a lower isotope composition. The similiarity of $\Delta^{34}S$, and consequently of equilibrium temperatures, of apatite and bulk rock of sample TS-12 implies that sulfur isotope equilibrium is still retained. Furthermore, the temperature of ~ 760 °C obtained from the sulfur fractionation in bulk rock and apatite of sample TS-12 conforms to geologically meaningful solidus temperatures in the range of 600–900 °C for barren porphyries (HUNT, 1991). This equilibrium has been disturbed during stage IV, as in sample SK-G1 a larger discrepancy between $\Delta^{34}S$ of apatite relative to bulk rock exists. A ~ 500 ppm difference in the sulfur content of both apatite from the unaltered and from the propylitically overprinted porphyry is assumed to be primary, as their SO_4^{2-}-derived/S^{2-}-derived sulfur ratios are essentially the same (23.8 and 25.9, respectively, c.f. Tab. 3). This may indicate that apatite with re-
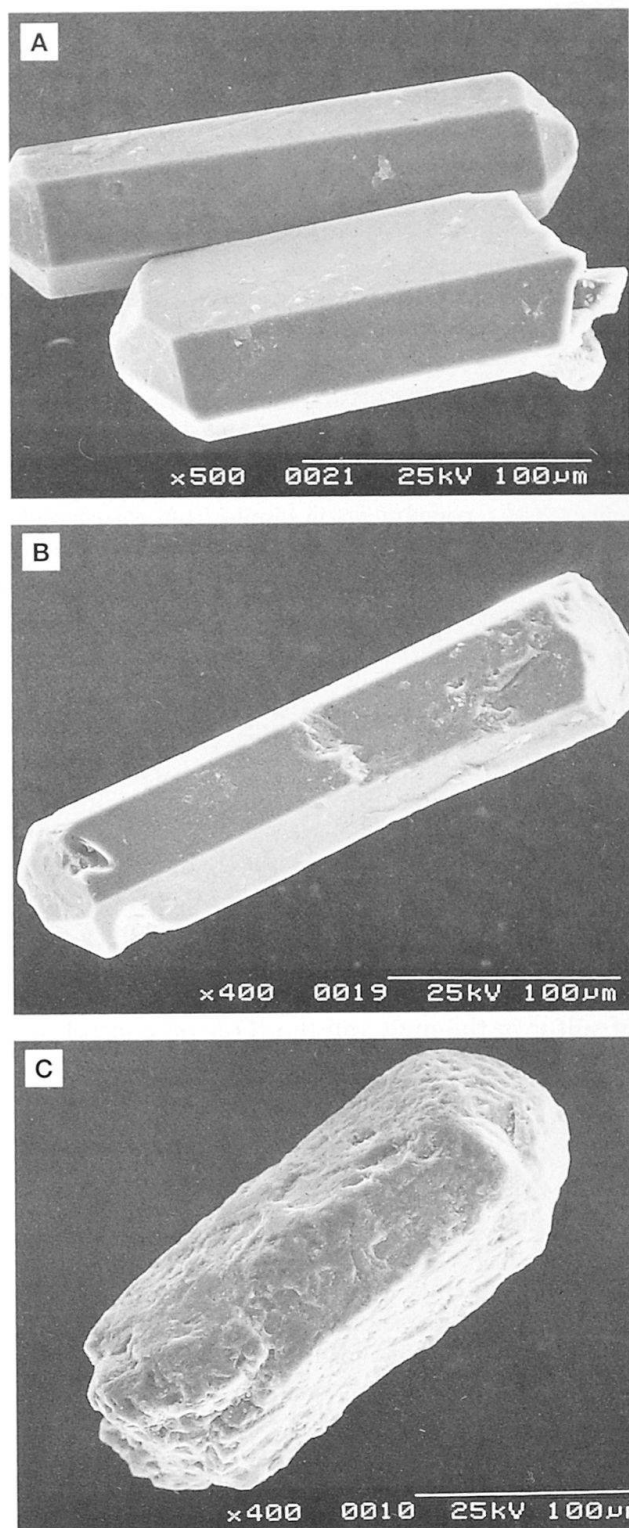
Fig. 4 REM-pictures of apatite crystals from the unaltered trachyte (A), the propylitically altered porphyritic syenite (B) from Skouries, and from the phyllically altered diorite porphyry at Fisoka (C). Skale bars correspond to 100 μm. Corrosive effects can only be observed in (C), whereas apatite in the other two cases preserved its shape under conditions prevailing during post-magmatic alteration.

spect to the sulfur isotope system is stable even under propylitic conditions. To elucidate this, REM-pictures of individual apatite crystals from sample TS-12 and SK-G1 have been made. They are presented in figure 4 together with a photograph of an apatite from the intensely phyllically altered diorite porphyry at Fisoka (Fig. 1). These photographs clearly show that major corrosive effects on crystal surfaces of apatite seem only to occur under phyllic alteration conditions, whereas under potassic and propylitic conditions apatite still preserves its idiomorphic crystal shape. The barren sample TS-12 is an example which demonstrates that mineralized trends in an intrusive suite may well be indicated by elevated sulfur concentrations (1791 ppm) in apatite.

Biotite solid solution from Skouries enabled the oxygen fugacitiy levels and temperature conditions to be traced during subsequent alteration stages. Temperatures calculated using the relations (2) and (3) are plotted against X_{phl} from biotite separated from the unaltered trachyte TS-12 (stage I), from the potassically altered porphyritic syenite sample SK-1 (stage II) and the propylitically overprinted sample SK-G1 in figure 5. Average data from the appropriate samples are listed in table 2. A series of equilibrium curves for the assemblage Fe-Mg-biotite + magnetite + san-
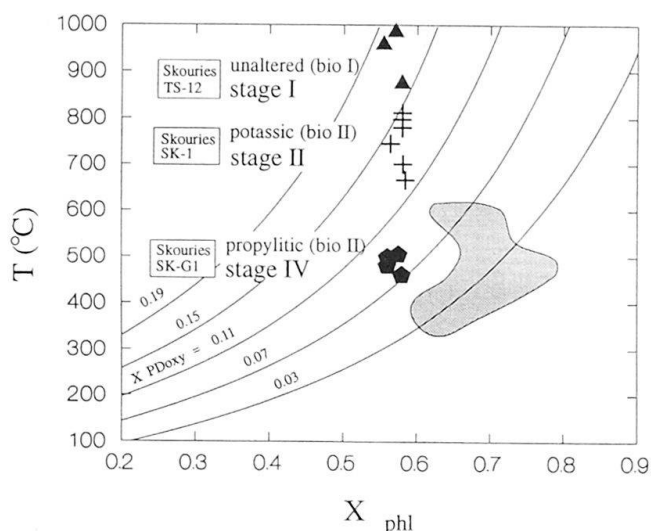

Fig. 6 T vs $\log fO_2$ diagram after BURNHAM (1980) with data of biotite from Skouries. Oxygen fugacities are estimated from the $\log fO_2$ vs T graph in figure 10 of JACOBS and PARRY (1979). Buffer lines for the system hematite (H) – magnetite (M) and fayalite (F) – quartz (Q) – magnetite (M) at ~ 1 kbar are plotted for reference purposes. Shaded fields mark the conditions typically prevailing in magnetite bearing I-type and S-type magmas and in porphyry Cu–Au deposits. Roman numbers (I, II, IV) correspond to the evolutionary stages at Skouries referred to in the text.

Fig. 5 X_{phl} vs T diagram with data of biotites (bio) formed during various hydrothermal stages in the porphyry copper intrusion of Skouries. A series of equilibrium curves for X_{PDoxy} between 0.03 and 0.19 are plotted for reference purposes. The shaded field comprises data of hydrothermal biotite from various porphyry copper deposits in the northwestern USA, i.e. from Bingham, Santa Rita, Ray, Safford, Rio Blanco, Hanover, El Teniente and Galore Creek (JACOBS and PARRY, 1979; KUSAKABE et al., 1990; and references cited therein).
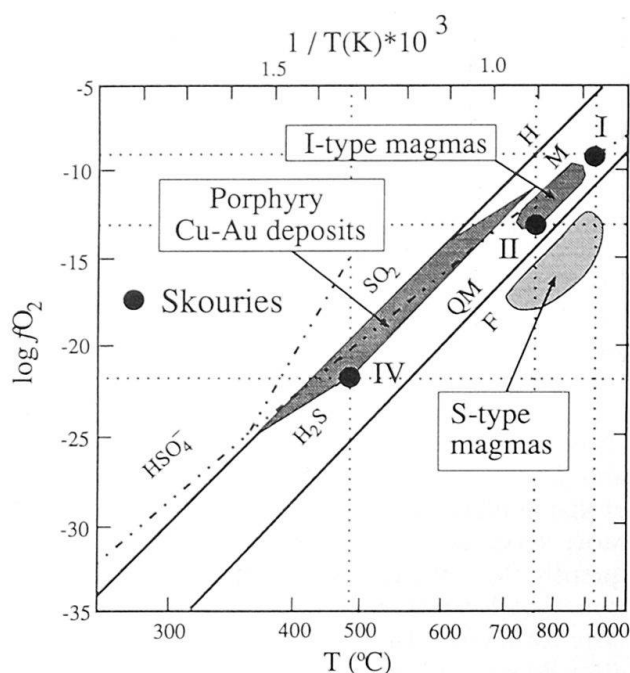
idine at fixed values of X_{PDoxy} are plotted as well. From the diagram in figure 5 it can be deduced that along with a temperature decrease from magmatic to propylitic conditions, biotite was depleted in X_{PDoxy}, whereas X_{phl} remained fairly constant. Consequently, the progressive depletion in X_{PDoxy} components is compatible with a continuous decrease in fO_2 during alteration. This trend is also depicted in figure 6, which is adapted from BURNHAM (1980) and slightly modified. Data of Skouries are consistent with $T–fO_2$ conditions in I-type magmas and porphyry Cu–Au deposits worldwide. However, as shown in figure 6, the initial fO_2 level in the magma must have been very high even under potassic conditions (stage II). Compared to data from other porphyry copper deposits (Santa Rita, Ray, Safford, Bingham, Hanover, Galore Creek; BEANE, 1974; JACOBS and PARRY, 1979; El Teniente, Rio Blanco; KUSAKABE, 1990), biotite solid solutions from Skouries are characterized by generally elevated X_{PDoxy} components. It is suggested that a major redistribution of Fe^{2+} and Fe^{3+} in secondary bio-

tite from Skouries occurred during stage IV (chloritization of edges). The calculated equilibrium temperature of ~ 490 °C should be carefully interpreted. It might at best indicate a maximum temperature for the stage IV hydrothermal overprint. Temperature conditions during this latest alteration stage have been independently estimated at ~ 210 °C using pyrite-chalcopyrite sulfur isotope fractionation (FREI, 1995). However, biotite solution data from Skouries are consistent with the general trend of decreasing Fe^{3+}/Fe^{2+} ratios from igneous to secondary biotite as observed in the Santa Rita porphyry, New Mexico (JACOBS and PARRY, 1979) and therefore are suitable for tracing the evolutionary path of the mineralizing fluid. Oxygen fugacity data can furthermore serve as base to estimate fH_2O and consequently P_{H_2O} at each stage, thus allowing estimation of hydrostatic pressures prevailing during biotite formation. The following simplified relation after WONES (1972) was used to compute approximate fH_2O values:

$$\log fH_2O = 7409/T + 4.25 + \frac{1}{2} \log fO_2 + 3 \log X_{ann} - \log a_{sanidine} - \log a_{mgt}$$

This relation is based on the assumption of a binary biotite solid solution, neglecting the trioctahedral Fe^{3+} substitution. The activities of sanidine and magnetite were taken as unity. Biotite solution data, temperatures and fO_2 values are listed in table 2. P_{H_2O} values were taken from tabulated values in BURNHAM et al. (1969). The following estimates were obtained:

– sample TS-12 fH_2O ~ 7100 bar, corresponding to P_{H_2O} of ~ 6 kbar,
– sample SK-1 fH_2O ~ 1900 bar, corresponding to P_{H_2O} of ~ 3 kbar,
– sample SK-G1 fH_2O ~ 40 bar, corresponding to P_{H_2O} of < 0.1 kbar, i.e. indicating near surface conditions.

The calculated pressures of ~ 6 and ~ 3 kbars from biotite solution data of samples TS-12 and SK-1, respectively, are high. According to BURNHAM (1979), water saturated magmatic bodies, from which typical copper porphyry systems develop, are emplaced in subvolcanic environments to depths of 2 to 5 km. Porphyry copper fracture systems are thus restricted to the uppermost few kilometers of the earth's crust, where the expansion of the H_2O-saturated carapace is large and where much of this expansion cannot be accommodated by plastic deformations of the roof rocks. At the early stage of a porphyry copper system, the melt becomes saturated with H_2O as the solidus is approached. During the crystallization of hornblende and biotite some H_2O is re-

moved from the melt, but generally only a small percentage can be removed in this fashion. Cooling of a melt that is saturated with water leads to the separation of a fluid phase by boiling, a process, during which heat is set free as a consequence of crystallization of one or more phases. This process is coupled with a volumetric expansion. This in turn is controlled by the total pressure, which in certain cases exceeds lithostatic load pressure. BURNHAM (1979) illustrates that extremely high internal overpressures can be generated in crystallizing hydrous magmas and theoretically can become infinitely high. In the opinion of this author, pressures practically can reach values of more than 5 kbars in isolated smaller pockets of H_2O saturated magma, such as for example in stocks and dikes. It is therefore assumed that the obtained pressures at which igneous biotite and biotite formed during potassic alteration at Skouries indicate hydrostatic overpressures (P_{H_2O}) rather than lithostatic pressure conditions. Further, the data indicate a marked internal pressure release to less than 50% of the initial value along with the onset of the late magmatic, potassic alteration. This effect is interpreted to be strongly coupled with the development of early fractures, creating outward and upward pathways for the fluid phase, i.e. extending the H_2O saturated carapace and consequently lowering the fluid pressure. This process continued during the early and late propylitic stages, during which earlier formed biotites were re-equilibrated. P_{H_2O} of < 0.1 kbar prevailed during the propylitic alteration and indicate that the fluid pressure was even lower than lithostatic pressures, mainly due to intense fracturing during the early propylitic stages (stage IIIA, IIIB), which allowed the escape of fluids.

The initially high fO_2 (slightly above the hematite-magnetite buffer) prevailing during the emplacement of the associated trachyte dike might have resulted from diffusive loss of H_2 during its emplacement in the subvolcanic environment. It is assumed, that prior to cooling of the magma below solidus temperatures volatiles generated during solidification of the magma above the solidus boundary escaped. Upon separation of an aqueous phase, reactions of the kind presented in the introductory chapter produce H_2. The immediate effect of this H_2 loss is an increase in fO_2 to maintain the $H_2O = H_2 + \frac{1}{2} O_2$ equilibrium. Since fO_2 normally is buffered by coexisting magnetite and ferromagnesian mineral such as hornblende, the effect of the fO_2 increase is that either hornblende changes composition (increase in ferric/ferrous ratio), or more likely, reacts with the melt to produce phlogopitic biotite, magne-

tite and plagioclase (BURNHAM, 1979). The same process also increases the production of SO_2, thus extracting sulfur from the melt. Cooling and ongoing crystallization in the parent stock caused the formation of a interstitial melt that became saturated with H_2O and encased the still largely molten interior of the stock. This "rind" prevented the escape of volatiles outward to the wallrocks. The decrease in fO_2 during the potassic and subsequent propylitic stages can be explained to result mainly from redox reactions of the fluid with ferromagnesian minerals such as hornblende or primary biotite. Reactions like the one presented below (BURNHAM, 1979) not only decreased the SO_2/H_2S ratio in the fluid and thus created ideal conditions for metal sulfide precipitation, but also decreased the fO_2, since the consumption of H_2O causes the equilibrium $H_2O = H_2 + \frac{1}{2}O_2$ to shift to the left side.

$SO_2 + 6$ "FeO" $+ H_2O \rightleftarrows H_2S + 3$ "Fe_2O_3"
"FeO" stands for ferrous iron bearing minerals (biotite, amphibole etc.)

Results from the study of ternary biotite solid solutions of Skouries indicate a marked decrease of the fO_2 from 10^{-10} to 10^{-22} during the emplacement and the onset of the potassic and the propylitic alteration of the porphyry. Initial emplacement of the trachyte is indicated at $\sim$ 940 °C. The oxygen fugacity during the crystallization of the trachyte biotites was high, i.e. slightly above the hematite-magnetite buffer. This is consistent with fO_2 in I-type magmas higher than the QFM buffer (BURNHAM and OHMOTO, 1989). Initially high fO_2 in porphyric intrusions therefore may be used as an indicator for an associated mineralization. This supports the conclusions by CHIVAS (1981) and MASON (1978), i.e. that increased oxygen fugacity levels in the melt can be equated with mineralizing trends if sufficient S, Cl and base metal is present in the magma and that in intrusive rocks associated with a mineralization, increasingly oxidizing conditions (increasing fO_2) in the melt result in successively different compositions of crystallizing ferromagnesian minerals. The potassic alteration was characterized by oxygen fugacity levels in the order of $fO_2 \sim 10^{-13}$ and temperatures of approximately 750 °C, which is in agreement with matrix quartz fluid inclusion homogenization temperatures in the range of 700–750 °C (TOMPOULOGLOU, 1981). The onset of a late, more localized and patchy propylitic alteration (stage IV) caused Fe^{2+}/Fe^{3+} redistribution in primary and secondary biotite. Under these conditions apatite was stable and maintained internal sulfur isotope equilibrium.

Conclusions

1. Sulfur concentrations in apatite can be used to distinguish barren from mineralized trends in intrusions emplaced within the SMM. S_{tot} concentrations below $\sim$ 1000 ppm are indicative of barren trends, whereas concentrations $> = 1000$ ppm point to intrusions which show a porphyry copper style mineralization or which are genetically associated with mineralized intrusions.

2. Bulk rock sulfur analyses have shown to be unreliable indicators of barren or mineralized trends. Weak alteration effects, mainly characterized by slight pyritization along with low temperature alteration specifically of mafic minerals, can drastically change the SO_4^{2-}-derived/S^{2-}-derived sulfur ratios and thus the sulfur isotope composition of the corresponding components. Consequently, and similar to Fe^{3+}/Fe^{2+} ratio of biotite, SO_4^{2-}-derived/S^{2-}-derived sulfur ratios of bulk rocks will not clearly distinguish barren from potentially mineralized intrusions in the SMM.

3. In contrast to bulk rock, apatite retains sulfur isotope equilibrium and is less sensitive to post-magmatic alteration. Due to its resilience, apatite can therefore potentially be used as an exploration aid to indicate possible mineralizing trends in intrusions.

4. The predominance of SO_4^{2-}-derived over S^{2-}-derived sulfur concentrations in bulk rock might be indicative of mineralized trends in intrusions. In at least two cases (the monzonite from Vathi; VATHI, and the porphyritic trachyte from Skouries; TS-12), in which oxidizing conditions are indicated by their bulk SO_4^{2-}-derived/S^{2-}-derived sulfur ratios, a genetic relation of the intrusions with porphyry copper mineralizations nearby is known. Because the porphyritic latite from Aspro Pighadi (AP-1) shows similar indications it would therefore be advisable to extend the exploration for related deposits in this area.

5. Biotite solid solution analyses are useful to determine approximate oxygen fugacity levels which prevailed during biotite formation and/or during their alteration. Due to the sensitivity towards mineral-internal redistribution processes with respect to Mg^{2+}, Fe^{2+} and Fe^{3+}, biotite solid solution data are indicators of post-magmatic disturbances. Deduced equilibrium temperatures may therefore signify maximum values at which redistribution took place.

6. The "Kiba"-method has shown to be a powerful technique to extract sulfur components not only from bulk rock, but also from apatite. With this technique trace sulfur amounts in the order of less than 45 μg ($\sim$ 0.4 μmol SO_2) can be volumetrically measured and subsequently, the sepa-

ration of the two gases allows isotope analyses to be performed on reduced and oxidized sulfur components.

References

AYRANCI, B. (1977): The major-, minor-, and trace-element analysis of silicate rocks and minerals from a single sample solution. Schweiz. Mineral. Petrogr. Mitt. 57, 299–312.

BANKS, N.G. (1982): Sulfur and copper in magma and rocks. In TITLEY, R. (ed.): Advances in geology of the porphyry copper deposits, The Univ. of Arizona press, Tucson, 227–257.

BEANE, R.E. (1974): Biotite stability in the porphyry copper environment. Econ. Geol. 69, 241–256.

BURNHAM, C.W. (1979): Magmas and hydrothermal fluids. In BARNES, H.L. (ed.): Geochemistry of Hydrothermal Ore Deposits, 2nd edition, J. Wiley and Sons, New York, 71–136.

BURNHAM, C.W. and OHMOTO, H. (1980): Late-stage processes of felsic magmatism: Soc. Mining Geol. Japan, Special Issue 8, 1–11.

BURNHAM, C.W., HOLLOWAY, J.R. and DAVIS, N.F. (1969): Thermodynamic properties of water to 1000 °C and 10'000 bars. Geol. Soc. Am. Spec. Paper 132, 96 p.

CARMICHAEL, I.S.E., TURNER, F.J. and VERHOOGEN, J. (1974): Igneous Petrology, New York, McGraw-Hill.

CHANNELL, J.E.T. and HORVATH, F. (1976): The African/Adriatic promotory as a paleogeographical premise for Alpine orogeny and plate movements in the Carpatho-Balkan region. Tectonophysics 35, 71–101.

CHIVAS, A.R. (1981): Geochemical evidence for magmatic fluids in porphyry copper mineralization. Part I. Mafic silicates from Koloula igneous complex. Contrib. Mineral. Petrol. 78, 389–403.

CHRISTOFIDES, G., D'AMICO, C., DEL MORO, A., ELEPHTERIADIS, G. and KYRIAKOPOULOS, C. (1990): Rb/Sr geochronology and geochemical characters of the Sithonia plutonic complex (Greece). Eur. J. Mineral. 2, 79–87.

CREASY, S.C. (1966): Hydrothermal alteration. In TITLEY, S.R. and HICKS, C.L. (eds): Geology of the porphyry copper deposits, southwestern North America: Tucson, Univ. Arizona Press, 51–74.

CZAMANSKE, G.K. and WONES, D.R. (1973): Oxidation during magmatic differentiation, Finnmarka Complex, Oslo area, Norway. Part 2. The mafic silicates. J. Petrol. 14, 349–380.

DE WET, A.P. and MILLER, J.A. (1987): ^{40}Ar–^{39}Ar data from some of the granitoids of the Chalkidiki peninsula, northern Greece. Abst. Joint meeting EUGS XII, 13–16 April, Strasbourg. Terra Cognita 7 (2–3), 107.

DEWEY, J.E., PITMAN, W.C., RYAN, W.B.F. and BONNIN, J. (1973): Plate tectonics and the evolution of the Alpine system. Geol. Soc. Am. Bull. 84, 3137–3180.

DIXON, J.E. and DIMITRIADIS, S. (1984): Metamorphosed ophiolitic rocks from the Serbo-Macedonian massif near Lake Volvi, north-east Greece. In DIXON, J.E. and ROBERTSON, A.H.F. (eds): The geological evolution of the eastern Mediterranean, Geol. Soc. London Spec. Publ. 17, 603–618.

ELIOPOULOS, D.G. and ECONOMOU-ELIOPOULOS, M. (1991): Platinum-group element and gold contents in the Skouries porphyry copper deposit, Chalkidiki peninsula, Northern Greece. Econ. Geol. 86, 740–749.

EUGSTER, H.P. and WONES, D.R. (1962): Stability relations of ferruginous biotite, annite. J. Petrol. 3, 82–89.

FILIPPIDIS, A., KOUGOULIS, C. and MICHAILIDIS, K. (1988): Sr-bearing stilbite in a quartz-monzonite from Vathi, Kilkis, northern Greece. Schweiz. Mineral. Petrogr. Mitt. 68, 67–76.

FOSTER, M.D. (1960): Interpretation of the composition of trioctahedral micas. U.S. Geol. Surv. Prof. Paper 354-B, 11–49.

FREI, R. (1992): Isotope (Pb, Rb–Sr, S, O, C, U–Pb) geochemical investigations on Tertiary intrusives and related mineralizations in the Serbomacedonian Pb– Zn, Sb + Cu–Mo metallogenetic province in Northern Greece. Unpubl. Ph. D. Thesis, ETH Zürich, Switzerland, 231 p.

FREI, R. (1995): The evolution of the mineralizing fluid in the porphyry copper system of Skouries, NE Chalkidiki; evidence from combined Pb–Sr and stable isotope data: Econ. Geol. 90, 746–762.

FYTIKAS, M., INNOCENTI, F., MANNETTI, P., MAZZUOLI R., PECCERILLO, A. and VILLARI, L. (1989): Tertiary to Quarternary evolution of volcanism in the Aegean region. J. Geol. Soc. London 22, 687–699.

GILG, H.A. (1993): Geochronology (K–Ar), fluid inclusion, and stable isotope (C, H, O) studies of skarn, porphyry copper, and carbonate hosted Pb–Zn (Ag, Au) replacement deposits in the Kassandra mining district (Eastern Chalkidiki, Greece). Unpubl. Ph. D. Thesis, ETH Zürich, Switzerland, 153 p.

GILG, H.A. and FREI, R. (1993): Chronology of magmatism and mineralization in the Kassandra mining area: implications for the potentials and limitations of dating hydrothermal illites. Geochim. Cosmochim. Acta 58, 2107–2122.

HEINRICH, E.W. (1946): Studies in the mica group: The biotite-phlogopite series. Am. Jour. Sci. 244, 836–848.

HOLLAND, H.D. (1967): Gangue minerals in hydrothermal deposits. In BARNES, H.L. (ed.): Geochemistry of hydrothermal ore deposits, New York, Holt, Rinehart and Winston, 382–436.

HUNT, J.P. (1991): Porphyry copper deposits. In HUTCHINSON, R.W. and GRAUCH, R.I. (eds): Historical perspectives of genetic concepts and case histories of famous discoveries. Econ. Geol. Monograph 8, 192–206.

JACOBS, D.C. and PARRY, W.T. (1979): Geochemistry of biotite in the Santa Rita porphyry copper deposit, New Mexico. Econ. Geol. 74, 860–887.

JANKOVIC, S. (1977): Metallogeny and plate tectonics in the northeastern Mediterranean. In DIMITRIJEVIC,

M. and GRUBRIC, A. (eds): Models of geotectonic development of the northeastern Mediterranean, Belgrade, 59–103.

JANKOVIC, S. (1978): The isotopic composition of lead in some Tertiary lead-zinc deposits within the Serbo-Macedonian Metallogenic Province (Yugoslavia). Geoloski anali balkanskoga paluostrua (Ann. géol. de la péninsule balkanique) 42, 507–525.

KALOGEROPOULOS, S.I., ECONOMOU, G.S., GEROUKI F., KARAMANOU, E., KOUGOULIS, C. and PERLIKOS, P. (1989): The mineralogy and geochemistry of the Stratoni granodiorite and its metallogenetic significance. Bull. Geol. Soc. Greece 23/2, 225–243.

KALOGEROPOULOS, S.I., KILIAS, S.P., BITZIOS, D.C., NICOLAOU, M. and BOTH, R.A. (1989): Genesis of the Olympias carbonate-hosted Pb–Zn(Au,Ag) sulfide ore deposit, Eastern Chalkidiki peninsula, Northern Greece. Econ. Geol. 84, 1210–1234.

KESLER, S.E., ISSIGONIS, M.J., ROWNLOW, A.H., DAMON, P.E., MOORE, W.J., NORTHCOTE, K.E. and PRETO, V.A. (1975): Geochemistry of biotites from mineralized and barren intrusive systems. Econ. Geol. 70, 559–567.

KIBA, T., TAKAGI, T., YOSHIMURA, T. and KISHI, I. (1955): Tin(II)-strong phosphoric acid; a new reagent for the determination of sulfate by reduction to hydrogen sulfide. Bull. Chem. Soc. Japan 28, 641–644.

KOCKEL, F., OLLAT, H. and GUNDLACH, H. (1975): Hydrothermally altered and (copper) mineralized porphyritic intrusions in the Serbomacedonian Massif (Greece). Mineral. Deposita 10, 195–204.

KONDOPOULOU, D. and WESTPHAL, M. (1986): Paleomagnetism of Tertiary intrusives from Chalkidiki (northern Greece). J. Geophys. 59, 62–66.

KUSAKABE, M., HORI M. and MATSUHISA, Y. (1990): Primary mineralization-alteration of the El Teniente and Rio Blanco porphyry copper deposits, Chile. Stable isotopes, fluid inclusions and $Mg^{2+}/Fe^{2+}/Fe^{3+}$ ratios of hydrothermal biotite. In HERBERT, H.K. and HO, S.E. (eds): Stable isotopes and fluid processes in mineralization, Geology Department and University Extension, the University of Western Australia Publication 23, 244–259.

MASON, D.R. (1978): Compositional variations in ferromagnesian minerals from porphyry copper-generating and barren intrusions of the Western Highlands, Papua New Guinea. Econ. Geol. 73, 878–890.

MIYOSHI, T., SAKAI, H. and CHIBA, H. (1984): Experimental study of sulfur isotope fractionation factors between sulfate and sulfide in high temperature melts. Geochem. J. 18, 75–84.

MOORE, W.J. and CZAMANSKE, G.K. (1973): Compositions of biotites from unaltered and altered monzonitic rocks in the Bingham mining district, Utah. Econ. Geol. 68, 269–280.

NEBEL, M.L., HUTCHINSON, R.W. and ZARTMAN, R.E. (1991): Metamorphism and polygenesis of the Madem Lakkos polymetallic sulfide deposit, Chalkidiki, Greece. Econ. Geol. 86, 81–105.

NEUBAUER, W.H. (1956): Der zyklische Magmatismus auf der Chalkidike und seine Erzlagerstätten. Berg- und Hüttenmännische Mh. 101, 164–169.

NEUBAUER, W.H. (1957): Geologie der blei-zinkreichen Kieslagerstätten von Kassandra (Chalkidike, Griechenland). Berg- und Hüttenmännische Mh. 102, 1–16.

NICOLAOU, M.N. (1960): L'intrusion granitic dans la région de Stratoni-Olympiade et sa relation avec la metallogenèse. Annales Géol. des Pays Hellénique 11, 214–265.

NICOLAOU, M.N. (1969): Recent research on the composition of the Kassandra Mines orebodies. Prakt. Akadem. Athens 44, 82–93.

NICOLOAU, M.N. (1964): The mineralogy and micrography of the sulfide ores of Kassandra Mines, Greece. Annales Géol. des Pays Hellénique 16, 111–139.

NIELSEN, J. (1979): Sulfur isotopes. In JÄGER, E. and HUNZIKER, J.C. (eds): Lectures in Isotope Geology, Springer Verlag, Berlin, 283–312.

OHMOTO, H. and RYE, R.O. (1979): Isotopes of sulfur and carbon. In BARNES, H.L. (ed.): Geochemistry of Hydrothermal Ore Deposits, J. Wiley and Sons, New York, 509–567.

PAPADAKIS, A. (1971): On the age of the granitic intrusion near Stratonion, Chalkidiki, Greece. Annales Géol. des Pays Hellénnique. 23, 297–300.

PAPADOPOULOS, G.A. and ANDINOPOULOS, A. (1984): Metallogenic evidence for palaeo-subduction zones in the Aegean area. Geologica Balcanica 14/4, 3–7.

PAVLIDES, S.B. and TRANOS, M.D. (1991): Structural characteristics of two strong earthquakes in the North Aegean: Ierissos (1932) and Agios Efstratios (1968). J. Struct. Geol. 13/2, 205–214.

SAKAI, H. (1968): Isotopic properties of sulfur compounds in hydrothermal processes. Geochem. J. 2, 29–49.

SAKELLARIOU, D. (1989): Geologie des Serbomazedonischen Massivs in der nordöstlichen Chalkidiki, N-Griechenland – Deformation und Metamorphose. Unpubl. Ph. D. Thesis, National and Kapodistrian Univ. of Athens, 177 p.

TOMPOULOGLOU, C. (1981): Les minéralisations Tertiaires, type cuivre porphyrique, du massif Serbo-Macédonien (Macédoine Grèce) dans leur contexte magmatique (avec un traitement géostatistique pour les données du prospect d'Alexia). Unpubl. Ph. D. Thesis, Ecole Nationale Supérieure des Mines de Paris, France, 204 p.

UEDA, A. and SAKAI, H. (1983): Simultaneous determination of the concentration and isotope ratio of sulfate- and sulfide-sulfur and carbonate-carbon in geological samples. Geochem. J. 17, 185–196.

VOIDOMATIS, PH.S., PAVLIDES, S.B. and PAPADOPOULOS, G.A. (1990): Active deformation and seismic potential in the Serbomacedonian zone, northern Greece. Tectonophysics 179, 1–9.

WONES, D.R. (1972): Stability of biotite: a reply. Am. Mineral. 57, 316–317.

WONES, D.R. and EUGSTER, H.P. (1965): Stability of biotite: Experiment, theory, and application. Am. Mineral. 50, 1228–1272.

ZACHOS, K. (1963): Discovery of a copper deposit in Chalkidiki peninsula, N-Greece. Geol. Geophy. Res. 8, 1–26.